Synthetic Map of Crop Leaf Area Index Dynamics Estimated with Satellite Data.

Robert FAIVRE[1] - Richard DELÉCOLLE[2]

[1] Biométrie et IA, INRA - Toulouse, BP 27, F 31326 Castanet-Tolosan Cedex, faivre@toulouse.inra.fr

[2] Bioclimatologie, INRA - Avignon, Site Agroparc, F 84914 Avignon Cedex, rdl@avignon.inra.fr

Abstract Monitoring crop growth or calibrating crop models with satellite remote sensing require too frequent data to rely on high space resolution satellites only. Coarse resolution satellites provide more frequent data, but their space resolution is too poor to allocate radiometric data to specific crops, specially when field size is comparatively small, as it is the case in West Europe agricultural systems. This paper proposes a scheme of use for such coarse data in the frame of the Preparatory Programme of VÉGÉTATION sensor to be launched. A map of land use is first derived from high resolution data (from SPOT satellite for instance) with all wavebands at few dates (generally three) and provides the percent cover of each crop in coarser pixels. Because the radiometric value in a coarse pixel is a weighted mean of the radiometric response of individual components, the reflectance of a specific crop inside each pixel is predicted by a model which unmixes coarse resolution values and reflectance of each crop is thus predicted at each available date of satellite observation. A time profile of Normalized Difference Vegetation Index (NDVI) is thus established for each crop. NDVIs being transformed into Leaf Area Indices (LAI), parameters of a simple model of time evolution of each crop can be estimated in each pixel with non linear regression. A synthesis of crop evolution can then be obtained when projecting values of estimated parameters on a map of the observed area. Knowledge of crop parameter distribution and space pattern at a regional scale is a first step to analyse the extension and behaviour of agricultural systems.

1 INTRODUCTION

Satellite monitoring of crops and crop yields requires information at an adequate space resolution and adequate time frequency. Space resolution must allow retrieval of crop-specific radiometric values (i) directly, with high-resolution scenes where elementary information (pixel) is significantly smaller (20x20 m^2 to 100x100 m^2) than agricultural fields ('pure pixels') and gives access to within-field variability, and to monitoring on a per-field basis, or (ii) indirectly with coarse resolution images where pixels (1 to 100 km^2) contain from several to many individual fields : the radiometric information in each pixel is then a mixture of elementary signals from elementary fields, *i.e.* a mixture of signals from various crops in most cases ('mixed pixels'). Time frequency of information is adequate if it gives access to important changes in crop behaviour. Changes in time profiles of crop state variables can be related to water or pathologic stresses or to ontogenetic events which in both cases are worth being considered. Unfortunately high ground resolution and high time frequency have so far been incompatible on present satellites. One is therefore compelled to retrieve ('unmix') crop-specific information from signals mixed in coarse pixels, using some indication on land use in these pixels as it is derived from scarce high-resolution scenes available over the same region (Fischer [1994]; Faivre and Fischer [1997]). Combining low- and high-resolution scenes from different platforms induces other negative by-products, such as lack of (i) radiometric compatibility (bandwidths are generally different) and (ii) geometric coherence (how accurate is superimposition of two images from different origins and resolutions?). A new platform to be launched in 1998 could partially overcome these drawbacks by operating a low-resolution sensor (VÉGÉTATION) and a high-resolution one (SPOT4) with common bandwidths and common geometry (at least in the centre of the swath). Such features are expected to improve the retrieval of frequent high-resolution information.

Another important issue is that adequate satellite monitoring of intensive agriculture requires both remotely sensed information and crop simulation models (Delécolle *et al.* [1992]). Incorporating satellite data into such models on a field basis has been reasonably well addressed at the moment, but methodologies for a regional approach are still to be produced, both because coarse resolution images must be used (cf. supra) and because crop models which would adopt regional inputs and preserve basic conditions for incorporating remotely sensed data do not still exist.

This paper is devoted to demonstrate methodologies to (i) unmix coarse resolution information and retrieve both mean values and variabilities of individual crop signals over a region and (ii) incorporate this information into a simple model of time evolution for leaf area index (which is a significant variables in crop models) and study the regional pattern of crop behaviour by mapping the values of the parameters in the model on a per-field basis.

2 DATA AND MAP OF LAND USE

Our methodologies were illustrated on a test-site where an adequate database is available, as established and described by Guérif *et al.* [1992]: the Camargue area. This is located in Southeast France and its approximate size is 15x10 km^2. During season 1986-1987, nine SPOT scenes were acquired in order to analyse the time evolution of optical characteristics for major crops in the area (wheat, rice, sunflower) in the visible and near-infrared wavebands. Normalised Difference Vegetation Index (NDVI) was computed on a pixel basis (20x20 m^2) from red and near infra-red reflectances provided by SPOT data. All pixels were classified into themes of land use (major crops, water, marshes, forest, others) by a maximum likelihood classification based on NDVI values for three dates. A segmentation of the agricultural area into agricultural fields was obtained by hand-drawing field contours from a high-scale map and comparing by eye with satellite scenes. A land use map on a field basis was derived from the two previous steps, as displayed in Figure 1.

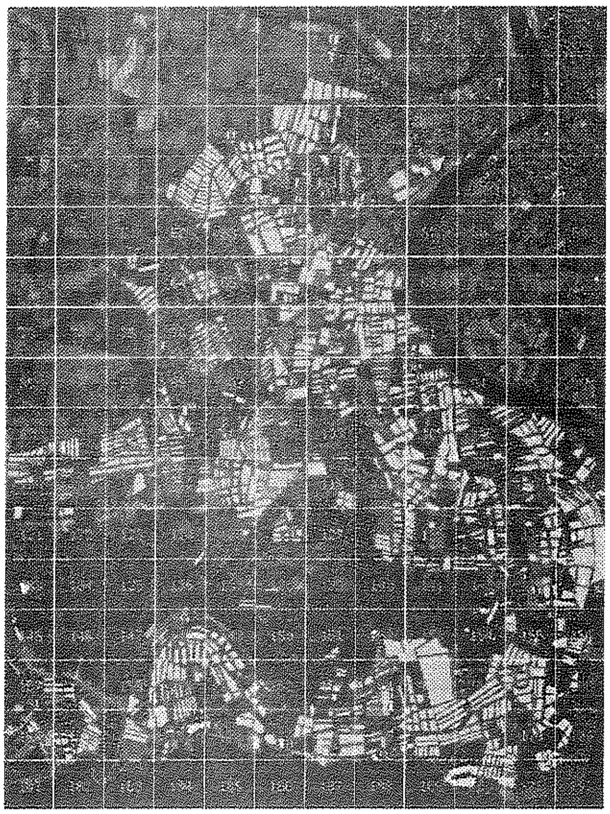

FIG. 1 - *Camargue land use map.*

A grid whose mesh size is the same as VÉGÉTATION pixels was identically drawn on each SPOT scene and VÉGÉTATION convolution kernels were used to compute red and infra-red synthetic reflectance per mesh. VÉGÉTATION pseudo-scenes were thus generated from initial SPOT scenes. A dataset was designed to contain (i) synthetic reflectances and derived NDVI at VÉGÉTATION scale and (ii) land use of each VÉGÉTATION pixel (percent area of each theme present in the pixel, as computed on a SPOT-pixel basis). Seven themes of land use were identified. Over the 192 VÉGÉTATION pixels, land use is: wheat (23 %), rice (17.8 %), sunflower (10.2 %), water (8.7 %), forests (11.4 %), cities (17.6 %), marshlands (11.3 %).

3 UNMIXING THE REFLECTANCE

Faivre and Fischer [1997] proposed a statistical modelling of such satellite data to predict information relative to crops observed through mixed pixels. At a given time and restricted to a homogeneous agro-climatic region, this model assumes that reflectances of the same theme (such as wheat, rice, forests, ...) are distributed as Gaussian with parameters depending on the theme. At each date and for each channel, conditional on the percentage of land occupation which is assumed to be known, we wrote a linear model with random components.

Let p be the number of themes, x_i^k be the proportion of theme k in pixel i, $\forall i \quad \sum_{k=1}^{p} x_i^k = 1$ and Y_i be the observed value on pixel i at one date and for one channel. If R_i^k is the unknown response of theme k in the pixel i, we model observed Y_i as

$$\left\{ \begin{array}{lcl} Y_i & = & \sum_{k=1}^{p} x_i^k R_i^k + \varepsilon_i \\ R_i^k & \sim & \mathcal{N}(\theta^k, \sigma_k^2) \end{array} \right. \tag{1}$$

where ε_i is the measurement error that we assumed to be identically and independently distributed: $\varepsilon_i \sim \mathcal{N}(0, \sigma_\varepsilon^2)$.

Under hypotheses of intra and inter pixel independences between R_i^k, parameters in model 1 were estimated using a maximum likelihood procedure. Figure 2 shows evolution of the three channels plus NDVI values for the seven components.

We then used the BLUP (Henderson [1975]), best linear unbiased prediction of the individual variations of reflectances inside the region. Conditional on the observed reflectance Y_i on the mixed pixel i, $\text{BLUP}(R_i^k)$ is, using the estimated variance parameters,

$$\widehat{R_i^k} = \widehat{\theta^k} + \frac{x_i^k \widehat{\sigma}_k^2}{\widehat{\sigma}_i^2} \left[Y_i - X\hat{\Theta} \right] \tag{2}$$

The deviations $Y_i - X\hat{\Theta}$ between observed and fitted values were decomposed into deviations due to the different themes depending on land use in the pixel and

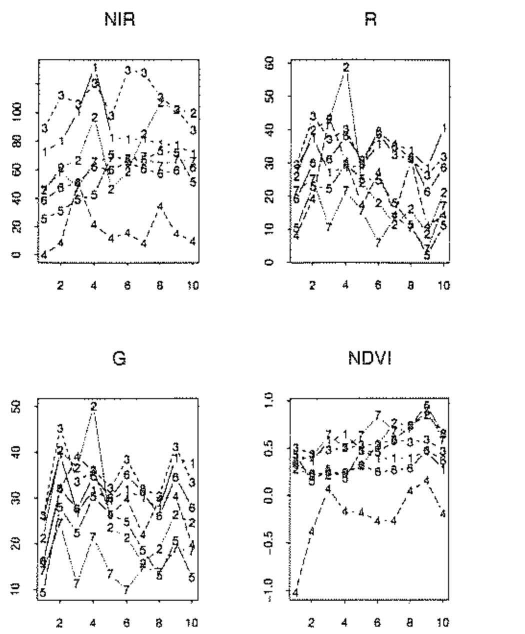

FIG. 2 - *Estimated profiles of numerical counts over the 10 dates for the 3 channels (near-infrared, red and green) plus* NDVI *and for the 7 themes: 1-wheat, 2-rice, 3-sunflower, 4-water, 5-forests, 6-cities, 7-marshlands.*

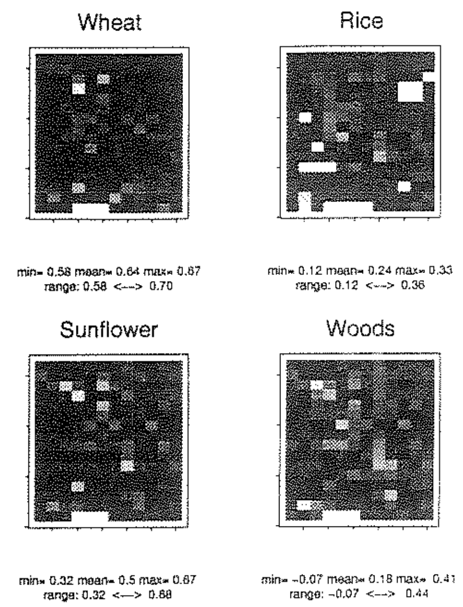

FIG. 3 - *Predicted map of* NDVI *on April, 15th for Wheat, Rice, Sunflower and Forests; highest values in black, lowest in white.*

on the natural variation of the themes over the image, the greater the percentage or the variance of the theme, the more important the correction (relative to the deviation).

For each date, for each channel and for each theme, a map of predicted values was drawn (Figure 3). $\widehat{\text{NIR}}$ and $\widehat{\text{R}}$ being the predicted numerical counts in the near-infrared and red wavebands, we calculated the corresponding predicted NDVI values as the ratio $\widehat{\text{NDVI}} = \frac{\widehat{\text{NIR}} - \widehat{\text{R}}}{\widehat{\text{NIR}} + \widehat{\text{R}}}$.

4 DYNAMIC MODELLING of CROP RESPONSE

For each pixel, it was then possible to analyse the evolution of predicted NDVIs for all themes. In the case of rice, Figure 4 illustrates an interesting feature of the results obtained for almost all themes. For several dates, NDVIs predicted at pixel level exhibited a range of values, as for the rest of time, predicted values were identical for all pixels. The explanation was to be found in the procedure of estimation. When a theme is not sufficiently variable (with respect to other components), σ_k^2 estimation is very close to 0. Thus, we predict for the rice at any pixel (see 2) the estimated mean value.

We used a canopy radiation transfer model for reproduce the interaction between crop vegetation canopy

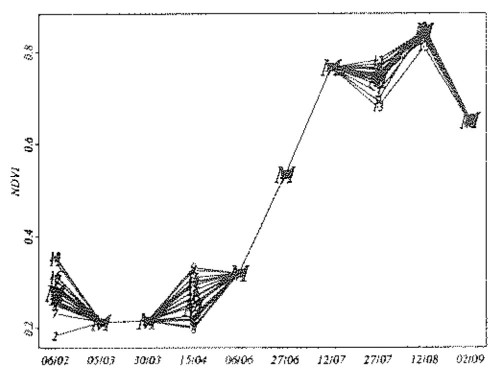

FIG. 4 - *Predicted profiles of* NDVI *for pixels where percent rice area is greater than 30 %; M stands for mean estimated value.*

and incoming radiation (only short wavelengths are addressed here) and thus allow to switch in both ways from canopy state variables (Leaf Area Index, LAI) to satellite-derived values (reflectances then Vegetation Indices NDVIs).

We use a conversion function g from LAI to NDVI $= g(\text{LAI}) = \text{NDVI}_{soil} + (\text{NDVI}_{max} - \text{NDVI}_{soil}) * (1 - e^{-\alpha * \text{LAI}})$ where α is an extinction coefficient depending on vegetation phase (from .94 during the green-up to .41 at senescence). In our condition, maximum vegetation index for rice is $\text{NDVI}_{max} = 0.9$, and soil index is $\text{NDVI}_{soil} = 0.15$.

LAI evolution described as a function of time was expressed in sum of degree-days and of different parameters. Baret [1986] used a summation of two exponential functions: a first one for the development phase and a second one for the senescence phase.

$$\text{LAI}(t, \beta) = k * \left[\frac{1}{1 + e^{-a*(t - t_i)}} - e^{b*(t - t_j)} \right]$$

with the constraint that $t_j = log(1 + exp(a * t_i))/b$ and $\beta^T = (k, a, b, t_i)$.

A least-square procedure was used to estimate parameter β. We have two possible objective functions. The first one is the sum of the mean squared errors calculated between observed predicted NDVI and fitted NDVI (as $g(\text{LAI})$). The second one is the sum of the mean squared errors calculated between observed predicted LAI (as $g^{-1}(\text{NDVI})$) and fitted LAI. We used a third one combining both strategies. The three objective criteria are:

$$\begin{aligned} C_{\text{NDVI}}(\beta) &= \sum_x \left[g(\text{LAI}(x, \beta)) - \widehat{\text{NDVI}(x)} \right]^2 \\ C_{\text{LAI}}(\beta) &= \sum_x \left[\text{LAI}(x, \beta) - g^{-1}(\widehat{\text{NDVI}(x)}) \right]^2 \\ C(\beta) &= C_{\text{LAI}}(\beta) + \tau \times C_{\text{NDVI}}(\beta) \end{aligned}$$

with $\tau = \frac{2}{[\text{NDVI}_{max} - \text{NDVI}_{soil}]^2}$. This estimation procedure was performed for each pixel.

5 RESULT ANALYSIS and DISCUSSION

Histograms of estimated parameter values are presented for rice in Figure 5. No special feature can be observed except the very concentrated distributions for the four parameters. This is not surprising because a large number of the 192 estimated values are very close. From these pixels, 16 did not contain any rice and almost one hundred contained less than 10 percent. Using correction formula (2), no or almost no correction was applied to the mean estimated value. So the rice predicted values were almost similar and as a consequence, the LAI parameters were identically estimated.

Considering pixels with high value of rice percent area, estimated parameters were quite different. Estimated

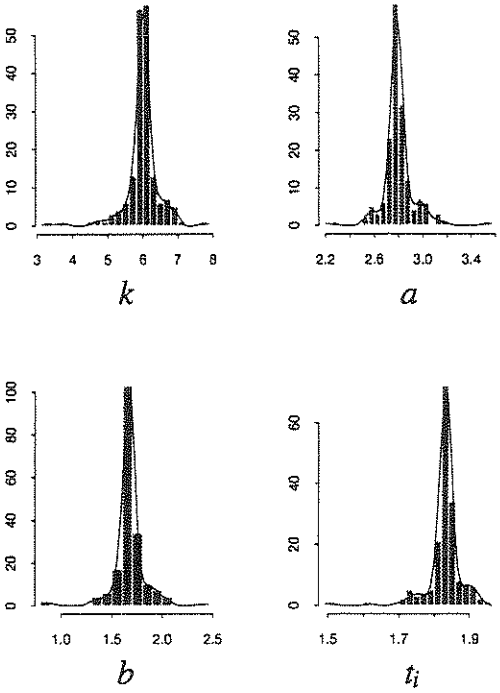

FIG. 5 - *Histograms of estimated parameter values for rice: counts in y-axis.*

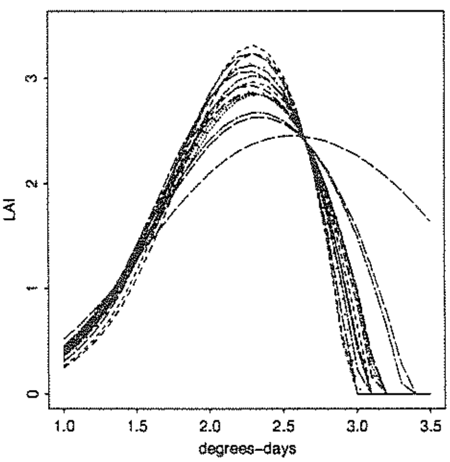

FIG. 6 - *Estimated curves of* LAI *as a function of degrees-days (x 1000) for pixels which contained least 30 % rice.*

shapes of LAI time profile are presented in Figure 6. LAI shape is highly sensitive to parameter values. A small variation in estimated value produces contrasted shapes. Meanwhile, estimation for the four parameters was done with only six dates. The precision of estimated parameters was low. We need a broader study with more measurement dates before any further conclusion.

Figure 7 displays maps of values for parameters (β) of the rice crop over the area. The space pattern of any parameter does not reveal strong structures, even if the Northern part of the area slightly contrasts with the Southern part by higher values of parameters K, a t_i and b, and lower values of parameter t_j. This can carefully be interpreted by more vigorous growth and earlier senescence, probably linked with earlier sowing dates, particular genotypes and/or specific fertilisation strategy. One can also observe that the space patterns of the first four parameters are very similar, revealing likely high empirical correlations between parameters which could question the real flexibility of our LAI time model. To validate or unvalidate our approach, we need to apply the same process to another region and/or theme where the range of agricultural practices is wider. An

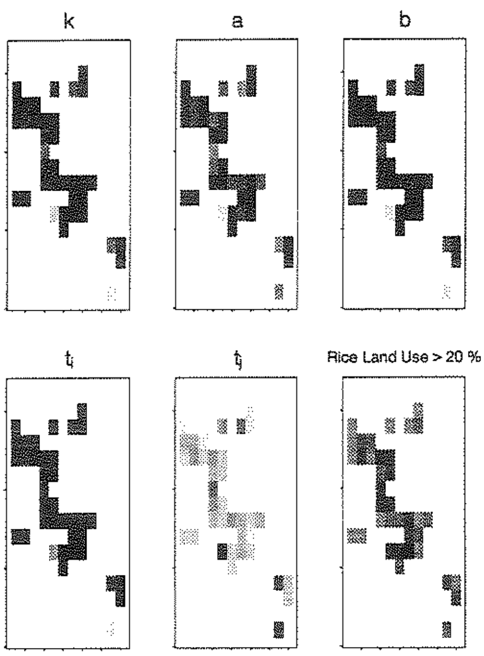

FIG. 7 - *Regional map of* LAI *estimated parameters and of rice land use for pixels which contained least 20 % rice.*

interesting issue of our approach could be to compare the results of LAI model calibration by using VÉGÉTATION and SPOT data respectively: VÉGÉTATION data are simulated from SPOT data. On Figure 8, we notice the randomness of SPOT data for the same agricultural field: is-it due to misclassification? Estimated time profile using VÉGÉTATION data agrees with estimated shapes based on SPOT data: VÉGÉTATION-based estimated time profile seems to be in the range of SPOT-based estimated profiles. Only one coarse pixel is presented here: a more complete analysis should be done.

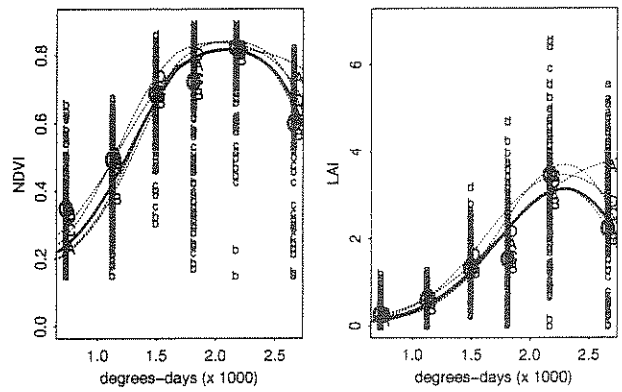

FIG. 8 - *Comparison between* SPOT *and* VÉGÉTATION *scales on the* NDVI *and* LAI *estimated curves. Unmixed* NDVI *and* LAI *values O and the corresponding estimated curves (solid and bold lines) for one coarse* VÉGÉTATION *pixel. Original* SPOT *data (small letters a, b, c and d) for the four agricultural rice fields within the same pixel. A, B, C and D correspond to the mean* SPOT *values and dotted lines to estimated curves.*

6 COMMENTS

From a statistical point of view, model (1) and prediction formula (2) can be improved by taking into account intra-pixel correlations of themes.

As we noticed above, estimated time profiles should be replaced by estimated confidence bands. Anyway a complete analysis should be done to point out information losses due to upscaling. An interesting work would be to appreciate the balance between gains in time frequency and losses in space resolution given by VÉGÉTATION sensor as compared to SPOT.

Nevertheless, our goal was to demonstrate a methodology to incorporate unmixed coarse resolution data into a simple model of time evolution at a regional scale. Sets of coefficient maps as exemplified by Figure 7 give a comprehensive view of crop behaviour in terms of space and time. They must be analysed vis-à-vis of the various knowledge of underlying high-resolution reality (land use as well as soil maps) and when compared with equivalent maps obtained at field scale from high-resolution scenes, they will help to quantify the effect of upscaling. They also are clues of homogeneity or patchiness of the observable resultant of some (genotype x environment

x crop management) interaction. In this sense, they are efficient tools for approaching, quantifying and describing the extension and intricacy of cropping systems over large areas.
Another way to interpret results of such multiple estimations is, regardless of their spatial pattern, to characterise the whole region by empirical distributions of values for each parameter and empirical covariances between parameters. The latter give information on possible links between agriculturally meaningful features (e.g. genotype earliness, sowing date, maximum development of vegetation, date of maturity), and can in turn be interpreted in terms of agricultural systems.

7 ACKNOWLEDGMENTS

Part of this work was subsidized by the VÉGÉTATION Preparatory Programme.

8 REFERENCES

Baret, F., Contribution au suivi radiométrique de cultures de céréales. Thèse d'Université, Université de Paris-Sud Orsay (France) 182pp, 1986.

Delécolle R., S.J. Maas, M. Guérif and F. Baret, Remote sensing and crop production models: present trends. ISPRS *Journal of Photogrammetry and Remote Sensing*, (**47**) 145-161, 1992.

Faivre R. and A. Fischer, Predicting crops reflectance using satellite data observing mixed pixels. *Journal of Agricultural, Biological, and Environmental Statistics*, Volume 2, Number 1, Pages 87-108, 1997.

Fischer A., A model for the seasonal variations of vegetation indices in coarse resolution data and its inversion to extract crop parameters. *Remote Sensing of Environment*, (**48**) 220-230, 1994.

Guérif, M., X. F. Gu and J. P. Guinot, Crop-System Characterization by Multitemporal SPOT Data in the South-East of France. *Int. J. Remote Sens.* 13(10): 1843-1851, 1992.

Henderson C.R., Best Linear Unbiased Estimation and Prediction under a selection model. *Biometrics* (**31**), 423-447, 1975.